

# MAGNETIC HYGIENE CONTROL ON LCLS-II CRYOMODULES FABRICATED AT JLAB\*

G. Cheng<sup>†</sup>, E. Daly, K. Davis, J. Fischer, N. Huque, B. Legg, H. Park, K. M. Wilson, L. Zhao,  
Thomas Jefferson National Accelerator Facility, Newport News, U.S.A.

## Abstract

Jefferson Lab (JLab) is in collaboration with Fermi National Accelerator Laboratory (Fermilab) to build 18 cryomodules to install at the SLAC National Accelerator Laboratory's tunnel as part of the Linac Coherent Light Source upgrade project (LCLS-II). Each LCLS-II cryomodule hosts 8 superconducting niobium cavities that adopt the nitrogen doping technique, which aims to enhance the cavity quality factor  $Q_0$  to reduce the consumption of liquid helium used to cool down the cavities. It is known that the  $Q_0$  of niobium cavities is affected by cavity surface magnetic field. Traditionally, magnetic shields made of high magnetic permeability  $\mu$ -metals are employed as a passive shielding of the ambient magnetic fluxes. During the LCLS-II cryomodule development, magnetic hygiene control that includes magnetic shielding and demagnetization of parts and the whole-machine is implemented. JLab and Fermilab worked closely on developing magnetic hygiene control procedures, identifying relevant tools, investigating causes of magnetization, magnetic field monitoring, etc. This paper focuses on JLab's experiences with LCLS-II cryomodule magnetic hygiene control during its fabrication.

## INTRODUCTION

The LCLS-II project adopts nitrogen-doped superconducting niobium cavities [1-2] for its potential to yield high  $Q_0$ , hence less heat load into the refrigeration system. Research has shown [2] that the doped cavities are more sensitive to surface magnetic field which causes surface resistance increase, compared to non-doped cavities. Hence, magnetic hygiene [3] control becomes necessary to preserve the high  $Q_0$  offered by doped cavities.

The LCLS-II specification [4-6] for the ambient magnetic field at cavity surface is  $< 5$  milligauss (mG) or  $0.5 \mu\text{T}$ . Fermi Lab and JLab are tasked to build thirty-five 1.3 GHz cryomodules (CMs). An increase in the number of modules to build is in planning. The two labs collaborate on magnetic hygiene control by implementing the same or equivalent procedures. Fermi's magnetic hygiene management has been summarized in the past [7]. This paper introduces JLab's practical experiences on implementing magnetic hygiene control.

## MAGNETIC SHIELDING

LCLS-II cryomodule's vacuum vessels (VV) are made

of ASTM A516 Grade 60 carbon steel that has the capability to attenuate geomagnetic field if the vessel is demagnetized [8-9]. JLab performs demagnetization on all LCLS-II VVs by use of a demagnetization system developed by Fermi Lab for LCLS-II. Figure 1 shows a typical attenuation from a demagnetized LCLS-II VV for a production CM. It is seen that in the majority of the VV's length, the magnetic field is lower than 50 mG. The production CM's VVs are heat treated at  $500^\circ\text{C}$  at the factory after welding and machining. The VV for prototype CMs (pCM) are not heat treated. JLab LCLS-II pCM VV after demagnetization shows higher than 50 mG magnetic field.

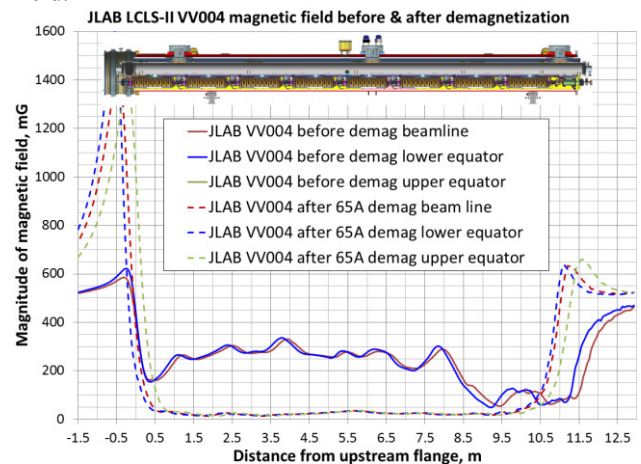


Figure 1: Magnetic field inside a LCLS-II VV post demagnetization.

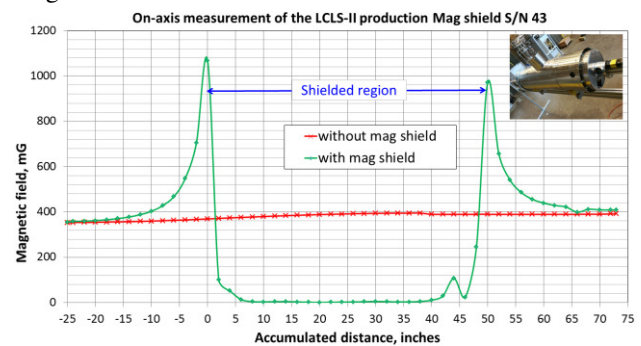


Figure 2: Mapped magnetic field inside a LCLS-II magnetic shield.

The LCLS-II CM adopts double-layer 1-mm thick Cryoperm 10<sup>®</sup> capped cylindrical magnetic shields [7] for each cavity. It has been discovered that such magnetic shields may have remnant magnetic field that may compromise their shielding performance. It is also well known that heat treatment can affect the permeability of magnetic shield materials. Therefore, an essential quality control step on the as-received magnetic shield is to perform field

\* Authored by Jefferson Science Associates, LLC under U.S. DOE Contract No. DE-AC05-06OR23177. The U.S. Government retains a non-exclusive, paid-up, irrevocable, world-wide license to publish or reproduce this manuscript for U.S. Government purposes. The work is supported by the LCLS-II project.

<sup>†</sup> cheng@jlab.org

Content from this work may be used under the terms of the CC BY 3.0 licence (© 2017). Any distribution of this work must maintain attribution to the author(s), title of the work, publisher, and DOI.

mapping inside a mock-up magnetic shield. Figure 2 shows the field mapping result on one representative magnetic shield. Note the field mapping is performed at room temperature and in geomagnetic field

Basing on the results from Figs. 1 and 2, it seems that a combination of a demagnetized carbon steel VV and double-layer magnetic shields will easily attenuate the geomagnetic field down below 5 mG and thus meet the project's specification. However, parts inside the magnetic shields and in between the magnetic shields and VV may have as-built residual magnetic field or develop magnetization during CM assembly. This then demands a systematic magnetic hygiene control that the LCLS-II CM project adopts.

## TOOLS AND INSTRUMENTATION

### Field Survey Tools

The magnetic hygiene control starts with parts surface magnetic field measurement. This is performed by use of 3-axis magnetometers. There is an old Chinese idiom "To do a good job, an artisan needs the best tools". Although there are various types of 3-axis magnetometers commercially available, it is not easy to find the best one. JLab, per Fermi Lab's recommendation, used Coliy G93<sup>®</sup> magnetometers to survey cavities and other parts. Then the G93 is found to be not durable and its reading can become unreliable after repeated usage. To replace or repair such a device is very slow and difficult. JLab also used Honeywell HMR2300<sup>®</sup> for some field survey. The drawback of HMR2300 seems to be that its housing induces an offset to the reading that may mislead the judgement on whether a part meets the specification or not. JLab is trying a few other types of magnetometers. What adds to the complexity is that while surveying a localized magnetic source, the orientation of the magnetometer affects the reading significantly. This can turn the field survey into a time-consuming process if an accurate reading is pursued.

For VV field mapping before and after demagnetization, JLab developed a motor-driven system that is based on JLab's cavity bead-pull measurement system, see Fig. 3. A Labview program is used to drive the motor and sample magnetic field data at a pre-set frequency.



Figure 3: Motor-driven VV magnetic field mapping system.

### Demagnetization Tools

For the VV, a 300-turn solenoid coil demagnetization system designed by Fermi Lab [3] is employed. To avoid winding/un-winding the 100-turn end coils repeatedly, JLab constructed a pair of mobile end coils, as shown in Fig. 4. The 300-turn coil system is also used to demagnetize CMs [10], as illustrated in Fig. 5. For the CM demagnetization, end coils are wound onto the Bayonet Box and End Cap, respectively. This demagnetization system may run at a maximum current of 65 A and is estimated [11] to be able to create 3000 G peak field inside the carbon steel wall of the VV. The system generates a relatively low peak field of 10 G along the centerline of the VV. Therefore for the low permeability parts inside the VV, if the magnetization is severe, the system may not be able to demagnetize them.



Figure 4: A mobile VV demagnetization 100-turn coil.

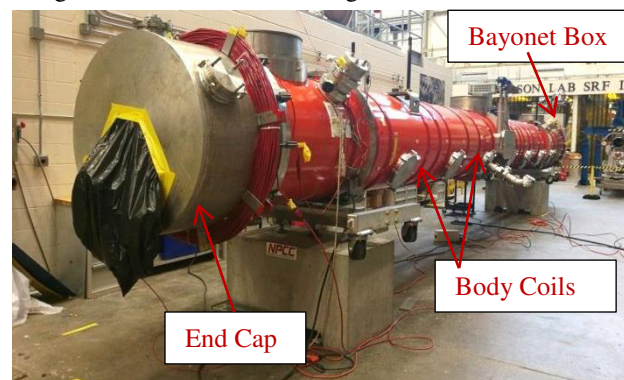


Figure 5: JLab LCLS-II pCM demagnetization.

For small parts, such as the Ti-SS joints on dressed cavities, clamps anchoring the helium vessels to a upper cold mass structure, tuner components, etc., JLab utilizes four types of demagnetizers: 1) a portable SPI Demagnetizer 98-269-4; 2) a DSC425-120 surface type demagnetizer; 3) a solenoidal demagnetizer run by a MPS Auto Degauss Model D220-40-3 console and 4) a 124-turn Helmholtz coil demagnetizer driven by approximately 15 A, 60 Hz AC current. The Helmholtz coil may generate a peak AC magnetic field of 370 G at edge and 83 G in the center. These demagnetizers are applied to various scenarios.

## Instrumentation

On the pCMs, the instrumentations that are relevant to magnetic hygiene monitoring include 13 Bartington single-axis fluxgate (FG) magnetometers [7] with Mag-F cryogenic probes and multiple temperature diodes affixed to cavity cells and magnetic shields. The 13 FGs, especially the 8 that are attached to cavity cells, are monitored during the fabrication, testing and transportation of JLab pCM. On the first few production CMs, only 5 FGs are installed in between the two layers of magnetic shields to serve as the “eyes” to guide potential in-situ active cancellation [10]. For each FG mounted on a cavity, there is an adjacent temperature diode. Readings from these temperature diodes are helpful in interpreting FG data during CM testing.

## MAGNETIZATION SOURCES

Superconducting niobium cavities are the core of a CM. At the early stage of the LCLS-II CM project, JLab discovered that the dressed (helium vessel welded-on) cavities present high magnetic fields at the titanium-stainless steel (Ti-SS) explosion bonded joints, as well as other small parts and welds on the dressed cavity.

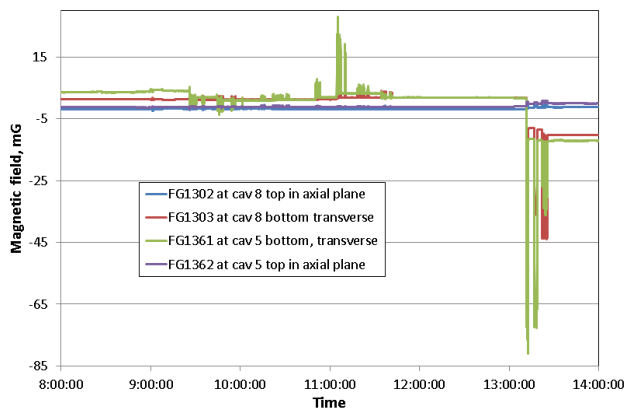


Figure 6: Influence of welding on cavity surface magnetic field.

Austenitic stainless steel parts theoretically shall be non-magnetic but in practice, the commonly used 304, 316 and 321 stainless steel parts are found to be magnetic. The LCLS-II team is well aware of this: therefore, specifications and procedures are developed to define components that need to be surveyed, and demagnetization is conducted on parts that fail to pass the initial evaluation. Near the completion of their pCM, Fermi Lab noted that a few FGs readings increased to as high as 46 mG [7]. JLab was then advised to pay attention to the FG reading changes caused by CM assembly, especially welding processes. Welders are requested to place the grounding clips as close to the weld as possible. Figure 6 shows the FG readings at the cavities 5 and 8 on the day when the final welding was carried out. As can be seen, the two transverse FGs experienced noticeable changes before and after welding. Both transverse FGs read roughly 8 mG higher after welding. The increase is much lower than what Fermi Lab’s pCM experienced. This shall be at-

tributed to JLab’s attention to where to ground when welding, per Fermi Lab’s advice.

During CM cool down and testing, thermocurrent and flux expulsion affect FG readings. More details and discussions are given in the following paragraphs.

## PROTOTYPE CRYOMODULE MAGNETIC FIELD TRACKING

The JLab pCM has been monitored throughout the fabrication stages and during the CM tests. To date, JLab pCM has been tested 3 times in December 2016-January 2017, April-May of 2017 and most recently in June of 2017, respectively. Figure 7 shows some FG data recorded. Note that:

- 1) The FGs are single-axis magnetometers so there are positive or negative numbers. The sign of the FG reading represents the orientation of localized magnet flux with respect to the axis of the magnetometer. For on-cell FGs, positive/negative sign is meaningful when investigating the flux expulsion behaviour as cavities cross niobium’s critical temperature  $T_{cr} = 9.25K$ . For FGs mounted on the magnetic shields, their signs are useful when orienting the applied active cancellation magnetic field.
- 2) FG readings above 5 mG are in red. However, these single-axis FGs actually only pick up one component of the local magnetic field. So, it is not conservative to compare these FG readings directly against the specification of < 5 mG, which means that the total magnitude shall be less than 5 mG. A conservative criterion would be <2.88 mG on each single axis FG, assuming the reading is duplicated in the other two orthogonal directions. On controlling the magnetic hygiene for the doped cavities that are sensitive to surface magnetic field, an As Low As Reasonably Achievable, i.e. ALARA, rule shall be observed [12].
- 3) The axial and transverse FGs on a certain cavity cell are positioned at top and bottom, respectively. Therefore, their readings cannot be used in vector sum to obtain total field magnitude. To date, there is no 3-axis magnetometer that can survive in cryogenic temperature.
- 4) The highlighted data are considered to be more of interest. The FG data after shipping test and before transitioning  $T_{cr}$  are highlighted. More discussions on shipping test and FG readings while transitioning are given in later paragraphs.
- 5) Please note the temperature and CM locations where the FG data are taken. In fact, when the pCM was outside of the JLab Cryomodule Testing Facility (CMTF), its longitudinal axis is 90 degrees in rotation from that of the pCM inside the CMTF. Plus, the JLab CMTF is shielded by multilayer mu-metals. When the CMTF is vacant, its field at LCLS-II beam line height was mapped and shown in Fig. 8.

Content from this work may be used under the terms of the CC BY 3.0 licence (© 2017). Any distribution of this work must maintain attribution to the author(s), title of the work, publisher, and DOI.

Cavity	Cell	position	orientation	FG#	11/30 right	11/30 pCM	Before pCM	after pCM	Before	after	After 2nd	pCM in CMTF	pCM before	pCM	pCM before
					before pCM	after 65A	cool down <sup>[2]</sup>	cool down	pCM shipping	shipping	65A	before re-	transitioning	before	transitioning
					11/30/2016	11/30/2016	12/14/2016	1/3/2017	2/22/2017	3/6/2017	4/7/2017	4/10/2017	5/2/2017	6/5/2017	6/11/2017
					R.T.	R.T.	R.T.	2-4K	R.T.	R.T.	R.T.	R.T.	13-25K	R.T.	R.T.
1	1	top	axial	1314	-5.10	4.26	2.77	-0.27	-0.12	-1.70	4.74	2.55	-0.36	0.86	0.41
1	1	bottom	transverse	1324	-8.40	1.29	0.78	0.92	-0.20	4.92	1.76	0.5	0.49	-0.42	0.86
4	1	top	axial	1369	0.94	3.96	1.44	-0.01	-7.29	4.69	3.2	0.33	-1.34	0.10	-0.83
4	1	bottom	transverse	1367	12.32	-1.88	-2.83	0.54	-0.43	-5.32	-2	-4.91	-0.66	-0.50	1.08
5	1	top	axial	1362	0.00	-3.45	0.68	-0.06	6.69	21.53	18.03	-10.89	-12.88	-7.42	-10.36
5	1	bottom	transverse	1361	-9.96	-2.31	-4.81	-4.69	-2.03	-3.94	-2.05	-4	-3.96	-0.13	-1.90
8	1	top	axial	1302	1.46	-1.02	-3.45	0.56	-0.80	-4.23	-4.42	2.54	5.41	2.30	5.00
8	1	bottom	transverse	1303	-8.67	-1.21	3.11	-0.04	-1.48	-2.54	-0.92	2.94	-0.93	2.33	0.26
1	Attached to the 2nd layer magnetic shields			1372			-9.23					-8.97		-1.97	
2	Axial FGs pointing upstream			1399			-5.95					-5.98		-0.82	
5				1402			-2.40					-3.67		-0.55	
7				1403			-1.24					-1.45		0.16	
8				1405			-2.53					-1.69		-0.85	

[1] pCM was outside of the CMTF and sitting on a pair of concrete blocks.

[2] pCM resides in the CMTF for testing

[3] pCM sits outside of the CMTF on a pair of concrete blocks that were slightly relocated from [1]. Blocks did not move when pCM is under shipping test.

Figure 7: JLab pCM fluxgate magnetometer recorded data (units are mG).

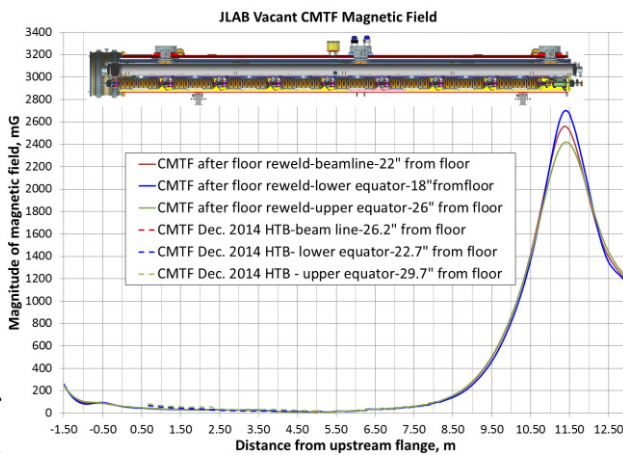


Figure 8: Magnetic field at LCLS-II CM beam line height in a vacant CMTF.

A few observations can be drawn from Figure 8 data:

- 1) Demagnetization on November 30, 2016 reduced the readings of 6 out of the 8 on-cell FGs. Two on-cell FGs experienced slight increases.
- 2) The low ambient field inside JLab CMTF does help to reduce the FG readings further.
- 3) After the first cool down in late December 2016, JLab pCM seems to have desirable low magnetic field on cavities that are equipped with FGs.
- 4) The pCM has undergone a shipping test [13] in late February, 2017. After the shipping test, a few on-cell FGs are seen to have increased readings. This indicates there is magnetization that happened during shipping. It is concerning because all LCLS-II CMs need to go through a long distance transportation to be delivered to SLAC. Jlab did try to demagnetize its pCM post shipping test at the maximum current, 65 A, twice. Limited mitigation on the FG readings is achieved.
- 5) CM cool down activates thermocurrents [10] that affect the magnetic field on the cavity cells, as manifested by the on-cell FG data. Jlab pCM has experi-

enced 3 cooldowns at different cool down rates. It is seen from the FG data that cool down rate affects generation of thermocurrents and thus the magnetic field on cavity surfaces.

- 6) When the cavities are transitioning  $T_{cr}$ , magnetic fluxes are expelled due to Meissner effect. The expelled magnetic fluxes affect the on-cell FG readings. Figure 9 shows the FG and on-cell temperature diodes, i.e. SRFTDs, readings during the most recent cooldown. As can be seen on June 11, 2017, there are abrupt changes on FG readings that can be attributed to flux expulsion while the cavities are transitioning to superconducting. It is said that fast cool down rate during the transitioning helps to enhance flux expulsion. That research topic is beyond the scope of this paper.

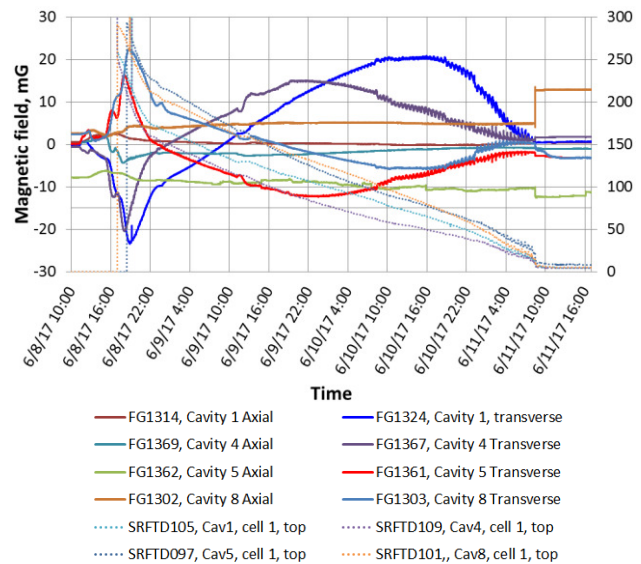


Figure 9: On-cell FG and diodes readings during the most recent JLab pCM cooldown.

The pCM magnetic hygiene would rather be judged by on-cell FG readings taken right before the moment when cavities transcend the  $T_{cr}$  since flux expulsion will change the magnetic field on the exterior surfaces of the cavities.

A good material expels flux well so it would be no surprise to see the on-cell FGs reading high post transitioning.

Just recently, JLab attempted to demagnetize its pCM inside the CMTF, where the ambient field is low, and when the cavities are cold, say 35K-ish temperature. The hope was that demagnetization can further improve the magnetic hygiene in the pCM. However, no improvements were obtained after trying to demagnetize twice at 65 A current. After all, there is only 10 G-ish degaussing field that is produced by the current demagnetization system. Data for these demagnetization attempts will be published separately.

## SUMMARY

JLab and Fermilab worked closely on implementing a systematic magnetic hygiene control to achieve high Q LCLS-II cavities. This is believed to be pioneering in large scale cryomodule fabrication projects. The efforts are rewarded by positive feedbacks from the magnetometers mounted on pCMs. Meanwhile, concerns over field survey tool and its reading, demagnetization tools, capability of the demagnetization system, etc. demand more investigations.

For LCLS-II CMs, the two pCMs are equipped with 13 FGs. Only 4 out of the 72 cavity cells, i.e. 5.6%, are monitored on the pCMs. Due to the cost of the cryogenic FGs, the production CMs do not have on-cell FGs installed. It is likely that only the eventual  $Q_0$  measurement, which by itself is tricky and affected by factors including but not limited to magnetic hygiene, will have the final say on whether magnetic hygiene helped on improving cavity performance or not.

## ACKNOWLEDGMENT

The authors would like to express our sincere acknowledgement to our JLab colleagues B. Carpenter, J. Follkie, D. Forehand, S. Lawrence, M. Murphy, L. Page, and A. Solopova for their help on the LCLS-II cryomodule magnetic hygiene control. We would also like to express our special thanks to S. K. Chandrasekaran and G. Wu from Fermi Lab and G. Ciovati, R. Geng and A. Palczewski from JLab for the valuable discussions and advice.

## REFERENCES

- [1] A. Grassellino et al., "Nitrogen and argon doping of niobium for superconducting radio frequency cavities: A pathway to highly efficient accelerating structures," *Supercond. Sci. Technol.*, vol. 26, 2013, No. 10, p. 102001, Aug. 2013.
- [2] D. Gonnella, "The fundamental science of nitrogen-doping of niobium superconducting cavities," Ph.D. dissertation, Cornell Univ., Ithaca, NY, USA, 2016.
- [3] G. Wu, "Overview on Magnetic Field Management and Shielding in High Q Modules," in Proc. SRF'15, Whistler, BC, Canada, Sep 2015, paper THBA06, pp. 1-6.
- [4] A. Romanenko and A. Crawford, "Magnetic Shielding: Requirements and Possible Solutions," LCLSII Engineering Note, LCLSII-4.5-EN-0222.
- [5] J. Theilacker, "1.3 GHz Superconducting RF Cryomodule," Functional Requirements Specification Document, LCLS-II-4.5-FR-0053.
- [6] T. Peterson, "1.3 GHz Cryomodule Technical Description," Engineering Specification Document, LCLS-II-4.5-ES-0356.
- [7] S. K. Chandrasekaran, A. Grassellino, C. Grimm, G. Wu, "Magnetic Field Management in LCLS-II 1.3 GHz Cryomodules," in Proc. LINAC'16, East Lansing, MI, USA, September 2016, paper TUPLR027, page 527-530.
- [8] A. Crawford, "A Study of Magnetic Shielding Performance of a Fermilab International Linear Collider Superconducting RF Cavity Cryomodule" <http://arxiv.org/abs/1409.0828>
- [9] M. Masuzawa, N. Ohuchi, A. Terashima, and K. Tsuchiya, "Study of Magnetic Shield for the STF Cryomodules," *IEEE Trans. Appl. Supercond.*, Vol. 18, No. 2, pp. 1423-1426, June 2008.
- [10] S. K. Chandrasekaran and A. C. Crawford, "Demagnetization of a Complete Superconducting Radiofrequency Cryomodule: Theory and Practice," *IEEE Trans. Appl. Supercond.*, Vol. 27, No. 1, p. 3500406, Jan. 2017.
- [11] S. K. Chandrasekaran, Hazard Form, Job Title "LCLS-II 1.3 GHz Cryomodule Demagnetization," unpublished.
- [12] S. K. Chandrasekaran, private communication, Jun. 2017.
- [13] N. Huque, E. F. Daly and M. McGee, "LCLS-II Cryomodule Transport System Testing," presented at SRF'17, Lanzhou, China, July 2017, paper MOPB109, this conference.